



Article

Hypomethylation of *CLDN4* Gene Promoter Is Associated with Malignant Phenotype in Urinary Bladder Cancer

Fumisato Maesaka ^{1,2,†}, Masaomi Kuwada ^{1,2,†}, Shohei Horii ¹, Shingo Kishi ¹, Rina Fujiwara-Tani ¹, Shiori Mori ¹, Kiyomu Fujii ¹, Takuya Mori ¹, Hitoshi Ohmori ¹, Takuya Owari ², Makito Miyake ², Yasushi Nakai ², Nobumichi Tanaka ², Ujjal Kumar Bhawal ^{1,3}, Yi Luo ⁴, Masuo Kondoh ⁵, Kiyohide Fujimoto ² and Hiroki Kuniyasu ^{1,*}

- ¹ Department of Molecular Pathology, Nara Medical University, 840 Shijo-cho, Kashihara 634-8521, Nara, Japan; mae_fumi0107@yahoo.co.jp (F.M.); masaomikuwada@gmail.com (M.K.); ngsoccer11n1212lv@gmail.com (S.H.); nmu6429@yahoo.co.jp (S.K.); rina_fuji@naramed-u.ac.jp (R.F.-T.); m.0310.s.h5@gmail.com (S.M.); toto1999-dreamtheater2006-sms@nifty.com (K.F.); pt_mori_t@yahoo.co.jp (T.M.); brahmus73@hotmail.com (H.O.); bhawal2002@yahoo.co.in (U.K.B.)
- ² Department of Urology, Nara Medical University, 840 Shijo-cho, Kashihara 634-8522, Nara, Japan; tinthereye@gmail.com (T.O.); makitomiyake@yahoo.co.jp (M.M.); nakaiyasusiuro@live.jp (Y.N.); sendo@naramed-u.ac.jp (N.T.); kiyokun@naramed-u.ac.jp (K.F.)
- ³ Department of Pharmacology, Saveetha Dental College, Saveetha Institute of Medical and Technical Sciences, Chennai 600077, India
- ⁴ Jiangsu Province Key Laboratory of Neuroregeneration, Nantong University, 19 Qixiu Road, Nantong 226001, China; lynantong@hotmail.com
- ⁵ Drug Innovation Center, Graduate School of Pharmaceutical Sciences, Osaka University, 6-1 Yamadaoka, Suita 565-0871, Osaka, Japan; claudindds@gmail.com
- * Correspondence: cooninh@zb4.so-net.ne.jp; Tel.: +81-744-22-3051; Fax: +81-744-25-7308
- † These authors contributed equally to this work.



Citation: Maesaka, F.; Kuwada, M.; Horii, S.; Kishi, S.; Fujiwara-Tani, R.; Mori, S.; Fujii, K.; Mori, T.; Ohmori, H.; Owari, T.; et al. Hypomethylation of *CLDN4* Gene Promoter Is Associated with Malignant Phenotype in Urinary Bladder Cancer. *Int. J. Mol. Sci.* **2022**, *23*, 6516. <https://doi.org/10.3390/ijms23126516>

Academic Editor: Roman Blaheta

Received: 10 April 2022

Accepted: 8 June 2022

Published: 10 June 2022

Publisher's Note: MDPI stays neutral with regard to jurisdictional claims in published maps and institutional affiliations.



Copyright: © 2022 by the authors. Licensee MDPI, Basel, Switzerland. This article is an open access article distributed under the terms and conditions of the Creative Commons Attribution (CC BY) license (<https://creativecommons.org/licenses/by/4.0/>).

Abstract: The tight junction (TJ) protein claudin-4 (CLDN4) is overexpressed in bladder urothelial carcinoma (BUC) and correlates with cancer progression. However, the mechanism of CLDN4 upregulation and promotion of malignant phenotype is not clear. Here, we analyzed 157 cases of BUC and investigated the hypomethylation of CpG island in the *CLDN4* promoter DNA and its correlation with cancer progression. In hypomethylated cases, CLDN4 expression, cell proliferation, stemness, and epithelial-mesenchymal transition were increased. Treatment of three human BUC cell lines with the demethylating agent aza-2'-deoxycytidine (AZA) led to excessive CLDN4 expression, and, specifically, to an increase in CLDN4 monomer that is not integrated into the TJ. The TJ-unintegrated CLDN4 was found to bind integrin $\beta 1$ and increase stemness, drug resistance, and metastatic ability of the cells as well as show an anti-apoptosis effect likely via FAK phosphorylation, which reduces upon knockdown of CLDN4. Thus, CLDN4 is overexpressed in BUC by an epigenetic mechanism and the high expression enhances the malignant phenotype of BUC via increased levels of TJ-unintegrated CLDN4. *CLDN4* promoter DNA methylation is expected to be a novel indicator of BUC malignant phenotype and a new therapeutic target.

Keywords: claudin-4; promoter methylation; bladder cancer; stemness; non-tight junction claudin

1. Introduction

Claudin-4 (CLDN4) is a major structural protein of epithelial tight junctions and is involved in epithelial differentiation, polarity maintenance, and substantial transport [1,2]. However, in epithelial malignancies overexpressing CLDN4, such as bladder urothelial carcinoma (BUC), colon cancer, gastric cancer, and pancreatic cancer, the barrier function of CLDN4 maintains the tumor microenvironment, retains growth factors, and protects tumors from intratumoral permeation of anti-cancer drugs [3–6]. CLDN4 expression is

correlated to cancer progression in these cancers [3–6]. The association of CLDN4 overexpression with carcinogenesis has also been suggested in pancreatic and ovarian cancers [7]. Interestingly, CLDN4 binds to integrins and promotes survival signals and stemness even when tight junctions are not formed [5]. In addition, reduced expression of CLDN4 in tumors is also associated with metastasis as they reflect epithelial-mesenchymal transition (EMT) [5,8]. Maintenance of the intratumor microenvironment by CLDN4 promotes malignant phenotypes in cancer through retention of growth factors and suppression of oxidative stress [3,9].

Epigenetic alterations play a major role in carcinogenesis and cancer progression in various malignancies [10–12]. DNA methylation, histone modifications, chromatin remodeling, and microRNA are considered useful indicators of cancer development and progression [13]. Epigenetic alteration in the regulation of CLDN4 expression has recently been reported. In gastric, bladder, and colorectal cancers, hypermethylation of the CpG sequence in the *CLDN4* gene promoter region leads to decreased CLDN4 expression [14–16]. In contrast, hypermethylation of the *CLDN4* gene and overexpression of CLDN4 have been reported in ovarian cancer [17]. In BUC, CLDN4 overexpression is associated with cancer progression [3]; however, its epigenetic status remains unclear. Therefore, in this study, we investigated the *CLDN4* promoter DNA methylation status and corresponding protein expression in BUC and examined its association with the malignant phenotype.

2. Results

2.1. DNA Methylation in the *CLDN4* Promoter in BUCs

The promoter region of the *CLDN4* gene contains several CpG sites, as shown in Figure 1A. In this study, we examined the methylation status of the CpG site located at the 1457 base pair (bp) upstream of the transcription start site (TSS). Methylation of this *CLDN4* promoter CpG site was examined using tissues from 157 BUC cases (Figure 1B–E, Table 1). The methylation rate in non-neoplastic bladder urothelium was $92 \pm 5\%$, whereas the BUC samples were significantly hypomethylated at $72 \pm 19\%$ ($p < 0.0001$). Furthermore, the methylation rate was lower in high-grade than in low-grade BUC (Figure 1B), and in the order of G3, G2, and G1 (Figure 1C, Table 1). With regard to wall invasion (pT factor) (Table 1), the methylation rate was lower in cases with subepithelial invasion (pT1) than in cases with non-invasive carcinoma (pTa), as well as lower in cases with muscle layer invasion (MIBC) than in cases with non-muscle layer invasion (NMIBC). When survival was examined in the top 50% (high methylation) and the bottom 50% (low methylation) groups, the overall survival was significantly poorer in the low methylation cases (Figure 1F). Thus, *CLDN4* hypomethylation correlated with BUC malignant phenotype.

Table 1. Methylation levels of promoter CpG of *CLDN4* gene in 157 BUC samples.

Parameter		<i>n</i>	Methylation (%)	<i>p</i>
Normal urothelium		20	92 ± 5	
BUC		157	72 ± 19	<0.0001
Grade ⁽¹⁾	G1	23	81 ± 12	
	G2	39	77 ± 24	
	G3	95	68 ± 20	0.0057
pT ⁽²⁾	pTa	61	82 ± 19	
	pTis	23	75 ± 20	
	pT1	34	73 ± 23	
	pT2	39	69 ± 23	0.0215
Muscle invasion	NMIBC	118	78 ± 21	
	MIBC	39	69 ± 23	0.0249

BUC, bladder urothelial carcinoma; CLDN, claudin; NMIBC, non-muscle invasion bladder cancer; MIBC, muscle invasion bladder cancer. ⁽¹⁾ Histological grade; G1, well differentiated; G2, moderately differentiated; G3, poorly differentiated according to TNM classification system [18]. ⁽²⁾ pT, primary tumor; pTa, non-invasive papillary urothelial carcinoma; pTis, carcinoma in situ; pT1, subepithelial invasion; pT2, muscle invasion according to TNM classification system [18].

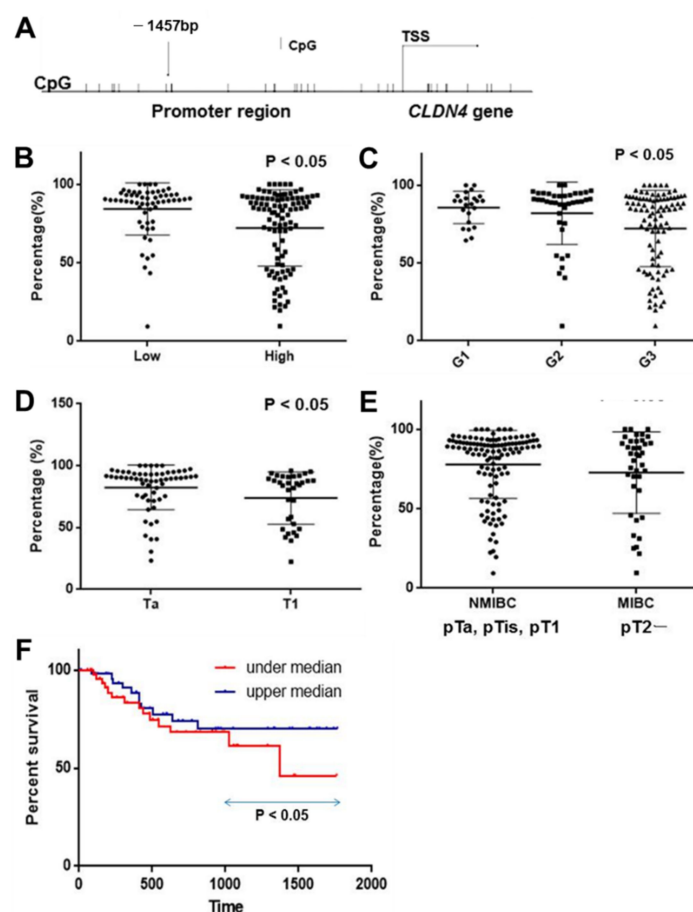


Figure 1. Hypomethylation of promoter DNA in *CLDN4* gene in 157 cases of BUCs. (A) Examined CpG island in *CLDN4* promoter region. (B) Comparison of *CLDN4* promoter methylation between low-grade and high-grade BUCs. (C) Comparison of *CLDN4* promoter methylation among G1, G2, and G3 BUCs. (D) Comparison of *CLDN4* promoter methylation between pTa and pT1 BUCs. (E) Comparison of *CLDN4* promoter methylation between NMIBCs and MIBCs. (F) Comparison of overall survival between *CLDN4* promoter methylation low (under median) and high (upper median) cases. Grade (high, low, or G1, G2, or G3) and primary tumor (pT; pTa, non-invasive papillary BUC; pT1, invasion into subepithelial layer) are classified according to the TNM classification system [18]. The data show the mean \pm SD, wherein the SD was calculated by Student's *t*-test. Survival analysis was performed by Kaplan–Meier method with statistical test by generalized Wilcoxon test. *CLDN*, claudin; BUC, bladder urothelial carcinoma; TSS, transcription starting site; percentage, frequency of CpG methylation; NMIBC, non-muscle invasive BUC; MIBC, muscle invasive BUC.

2.2. *CLDN4* Promoter DNA Methylation and Gene Expression

Next, we examined *CLDN4* promoter methylation and expression of *CLDN4*, stem cell-related genes, and EMT-related genes in 23 invasive BUC samples from the above 157 cases from which mRNA extraction was possible. The comparison of the clinicopathological factors and *CLDN4* promoter methylation among the 23 cases is shown in Table 2. The hypomethylated cases showed an infiltrative invasive pattern of cancer, greater frequency of vascular invasion, and more local recurrences than the hypermethylated cases. In terms of gene expression, the hypomethylated cases showed higher *CLDN4* expression and proliferative activity (Ki-67) compared to the hypermethylated cases (Figure 2A). The stemness markers *GNL3* and *CD44v9* showed higher expression in the hypomethylated cases than in the hypermethylated cases. Among the EMT-related genes, *CDH1* expression was decreased while that of *SNAIL* and vimentin was increased in the hypomethylated cases compared to the hypermethylated gene cases. Immunostaining confirmed that these

changes at the mRNA level were also reflected at the protein level (Figure 2B). Thus, *CLDN4* hypomethylation was associated with increased *CLDN4* expression, stemness, and EMT induction in BUC.

Table 2. Comparison of pathological parameters between *CLDN4*-methylation high and low cases.

Parameter	CLDN4 Methylation ⁽¹⁾		<i>p</i>
	High	Low	
Number	11	12	
Grade ⁽²⁾			
	Low	0	NS
	High	10	
pT ⁽³⁾			
	pT1	10	NS
	pT2	1	
INF ⁽⁴⁾			
	a/b	11	0.0046
	c	0	
Ly/V ⁽⁵⁾			
	-	11	0.0006
	+	0	
Reurrence ⁽⁶⁾			
		3	0.0123

⁽¹⁾ Methylation high, cases belonging to the upper 50% of methylation percentage; methylation low, cases belonging to the lower 50% of methylation percentage. ⁽²⁾ Histological grade low, G1-2; high, G3 according to TNM classification system [18]. ⁽³⁾ pT, primary tumor; pT1, subepithelial invasion; pT2, muscle invasion according to TNM classification system [18]. ⁽⁴⁾ INF, tumor infiltrative pattern into the surrounding tissues; INFa, expanding growth with a distinct border; INFb, intermediate pattern between INFa and INFc; INFc, infiltrative growth with no distinct border. ⁽⁵⁾ Ly/V, capillary invasion; Ly, lymphatic invasion; V, venous invasion. ⁽⁶⁾ Recurrence, local recurrence after transurethral resection.

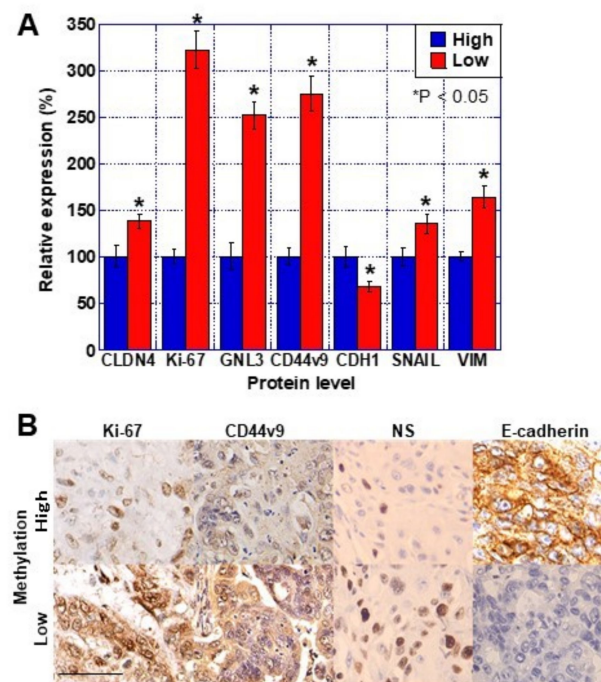


Figure 2. Levels of malignant phenotype-associated proteins in 23 cases of BUCs. Protein expression in the 23 BUC cases shown in Table 2 (11 high-methylation and 12 low-methylation cases) were examined by (A) ELISA and (B) immunohistochemistry. Relative protein levels of *CLDN4*, Ki-67 (proliferation), *GNL3* and *CD44v9* (stemness), and *CDH1*, *SNAIL*, and vimentin (EMT). Error bar indicates the SD calculated by Student's *t*-test. Scale bar, 50 μ m. *CLDN*, claudin; BUC, bladder urothelial carcinoma; *VIM*, vimentin; EMT, epithelial-mesenchymal transition.

2.3. Effects of *CLDN4* Promoter DNA Demethylation

The results indicated that the *CLDN4* promoter DNA is hypomethylated in BUC. Next, we treated three human BUC cell lines with the demethylating agent aza-2'-deoxycytidine (AZA) and examined its effects (Figure 3). In BUC cells, AZA treatment reduced *CLDN4* promoter DNA methylation rate to approximately 50%. Furthermore, *GNL3*, the stemness marker, and *BCL2*, the anti-apoptotic factor, were upregulated, while *BAX*, the pro-apoptotic factor, was downregulated upon AZA treatment (Figure 3B).

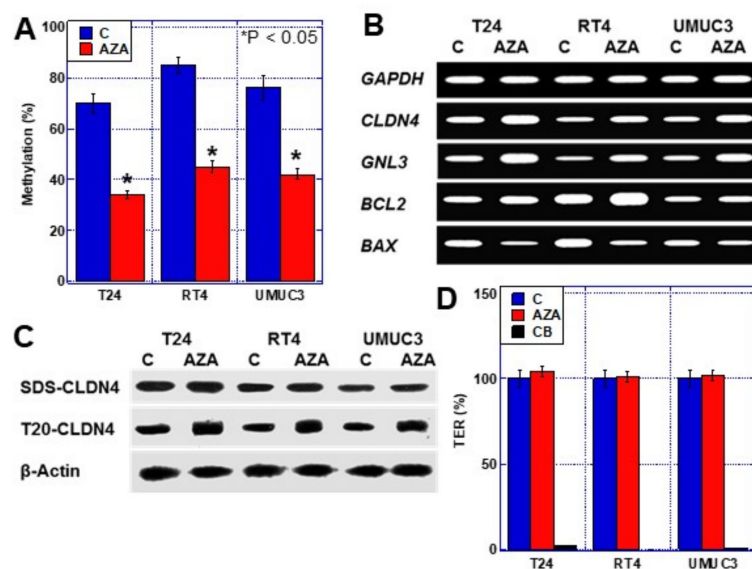


Figure 3. Effect of AZA treatment in three human BUC cells. (A) Frequency of methylation of *CLDN4* promoter in T24, RT4, and UMUC3 human BUC cells with or without AZA treatment. (B) Effect of AZA on mRNA expression. (C) Effect of AZA on *CLDN4* protein expression and tight junction integrity in T24 cells. (D) Effect of AZA on TER in T24 cells. Error bar indicates SD calculated by Student's *t*-test. CLDN, claudin; BUC, bladder urothelial carcinoma; AZA, 5-aza-2-deoxycytidine; SDS-CLDN4, 0.5% sodium dodecyl sulfate-solubilized *CLDN4* (whole *CLDN4*); T20-CLDN4, 0.5% Tween 20-solubilized *CLDN4* (tight junction unintegrated *CLDN4*); TER, transepithelial electrical resistance; CB, cytochalasin B.

Examination of the protein level of whole *CLDN4* (sodium dodecyl sulfate-solubilized *CLDN4*; SDS-CLDN4) following increased expression of *CLDN4* mRNA by AZA treatment showed no change (Figure 3C). In contrast, protein levels of tight junction-unintegrated *CLDN4* (Tween 20-solubilized *CLDN4*; T20-CLDN4) were increased in the three types of BUC cells. Furthermore, when the function of the tight junction was examined by transepithelial electric resistance (TER) assay, the TER was not found to be altered by AZA treatment (Figure 3D). Thus, excess *CLDN4* expression by *CLDN4* promoter DNA hypomethylation increased only the T20-CLDN4 levels and promoted stemness and anti-apoptotic survival.

2.4. Effects of *CLDN4* Knockdown

Next, *CLDN4* was knocked down by short interference RNA (siRNA), and its effects were examined (Figure 4). *CLDN4* knockdown resulted in a decreased expression of *CLDN4*, stemness marker *GNL3*, and anti-apoptotic factor *BCL2*, and increased expression of the pro-apoptotic factor *BAX* (Figure 4A). In addition, *CLDN4* knockdown decreased the sphere-forming ability of the cells, indicating decreased stemness (Figure 4B). Further, we changed the *CLDN4* expression levels in T24 cells using various siRNA concentrations, followed by measurement and comparison of the levels of SDS-CLDN4 and T20-CLDN4 and TER (Figure 4C,D). The 2 μ M siRNA treatment reduced T20-CLDN4, whereas SDS-CLDN4 levels were largely unchanged and ZO-1-bound *CLDN4* levels were preserved.

In this knockdown condition, no significant decrease was observed in TER. In contrast, 5 μ M siRNA treatment decreased SDS-CLDN4 and ZO-1-bound CLDN4 levels, along with a decrease in TER. Thus, T20-CLDN4 was not linked to tight junction function, implying that it might be the excess relative to the amount of CLDN4 that is required to maintain tight junction function.

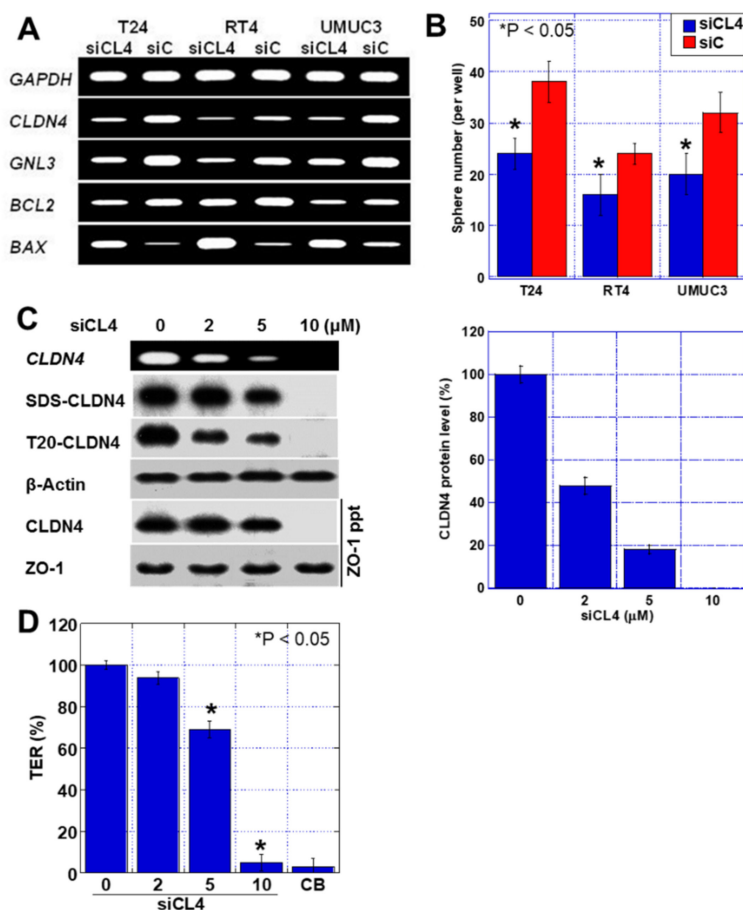


Figure 4. Effect of *CLDN4* knockdown in three human BUC cells. (A) Effect of *CLDN4* knockdown on mRNA expression. (B) Effect of *CLDN4* knockdown on sphere formation. (C) Effect of *CLDN4* knockdown on *CLDN4* expression and tight junction integrity. (Right) Semi-quantification of *CLDN4* protein levels in siCL4-treated T24 cells. (D) Effect of *CLDN4* knockdown on TER in T24 cells. Error bar indicates SD calculated by Student's *t*-test. CLDN, claudin; BUC, bladder urothelial carcinoma; si, short interference RNA; siC, control siRNA; siCL4, siRNA for *CLDN4*; SDS-CLDN4, 0.5% sodium dodecyl sulfate-solubilized *CLDN4* (whole *CLDN4*); T20-CLDN4, 0.5% Tween 20-solubilized *CLDN4* (tight junction unintegrated *CLDN4*); ppt, immunoprecipitant; TER, transepithelial electrical resistance; CB, cytochalasin B.

2.5. Non-Tight Junction *CLDN4* Binding to Integrin β 1

We previously reported that *CLDN4* acts as a ligand for integrin β 1 and is involved in the subsequent signal formation [5]. Here, we examined the association between *CLDN4* and integrin β 1 in T24 cells (Figure 5). The levels of *CLDN4*-bound integrin β 1 and phosphorylated FAK both decreased upon knockdown of *CLDN4*. Next, we examined binding of integrin β 1 to T20-*CLDN4* and tight junction-integrated *CLDN4* (perfluorooctanoic acid-soluble *CLDN4*; PFO-*CLDN4*) and confirmed that it binds only to T20-*CLDN4* (Figure 5B,C). In the case of PFO-*CLDN4*, dimer, trimer, and tetramer were extracted along with the monomer (Figure 5B). In contrast, extraction of T20-*CLDN4* showed only the monomer. When this extract was mixed with recombinant integrin β 1 and incubated for

binding, only the CLDN4 monomer bound to integrin β 1 (Figure 5C). Since the binding of CLDN7 to integrin β 1 has been reported [19], the binding of integrin β 1 with CLDN4 and CLDN7 was compared (Figure 5D). The affinity between integrin β 1 and CLDN4 was found to be approximately 40% of that observed with CLDN7.

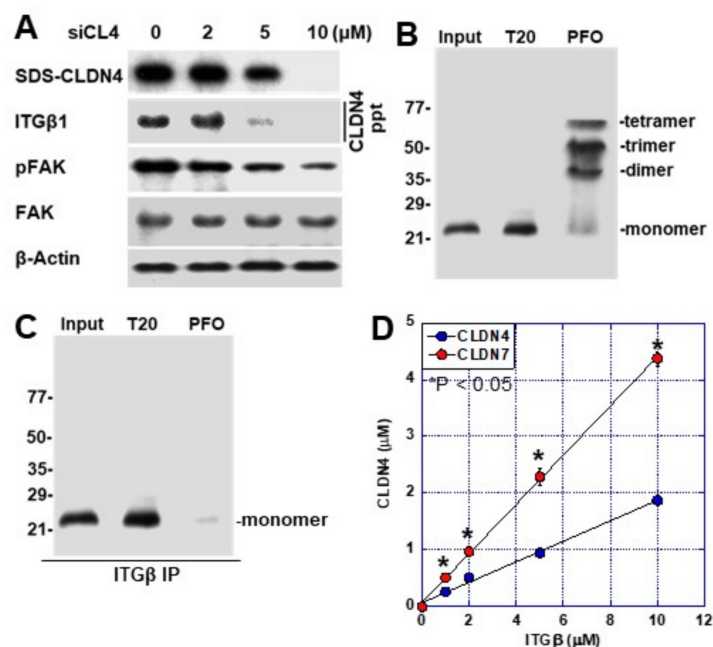


Figure 5. Physical association between CLDN4 and integrin β 1 in T24 cells. (A) Effect of *CLDN4* knockdown on CLDN4–ITG β 1 binding and FAK phosphorylation. (B) CLDN4 detected by immunoblotting using 0.5% Tween 20-solubilized lysate (T20) or 0.5% perfluoro-octanoic acid-soluble lysate (PFO). (C) CLDN4 bound to ITG β 1 detected by immunoprecipitation. (D) Comparison of the affinity to ITG β 1 between CLDN4 and CLDN7. Error bar indicates SD calculated by Student’s *t*-test from three independent trials. CLDN, claudin; BUC, bladder urothelial carcinoma; si, short interference RNA; siC, control siRNA; siCL4, siRNA for CLDN4; ITG β 1, integrin β 1; FAK, focal adhesion kinase; pFAK, phosphorylated FAK. SDS-CLDN4, 0.5% sodium dodecyl sulfate-solubilized CLDN4 (whole CLDN4); T20, 0.5% Tween 20-solubilized CLDN4 (tight junction unintegrated CLDN4); PFO, 0.5% perfluoro-octanoic-solubilized CLDN4 (tight junction integrated CLDN4); ppt, immunoprecipitant.

2.6. Effects of Integrin Activation by CLDN4

Finally, the effect of integrin β 1 activation by CLDN4 was examined in T24 cells (Figure 6). We examined the effects on sphere formation and apoptosis in a *CLDN4* knockdown system (Figure 6A,B). Upon decreasing *CLDN4* expression by knockdown, the sphere volume decreased while apoptosis increased. Knocking down integrin β 1 resulted in greater changes in both sphere formation and apoptosis than *CLDN4* knockdown (Figure 6C). Furthermore, knockdown of *CLDN4* increased the sensitivity of the cells to the drug cisplatin (CDDP) (Figure 6D). In a subcutaneous mouse tumor model, CDDP suppressed tumor growth after *CLDN4* knockdown, whereas increasing *CLDN4* expression by AZA treatment enhanced tumor growth. In a mouse model of lung metastasis induced by tail vein inoculation, *CLDN4* knockdown suppressed lung metastasis, whereas increasing *CLDN4* expression by AZA treatment enhanced lung metastasis.

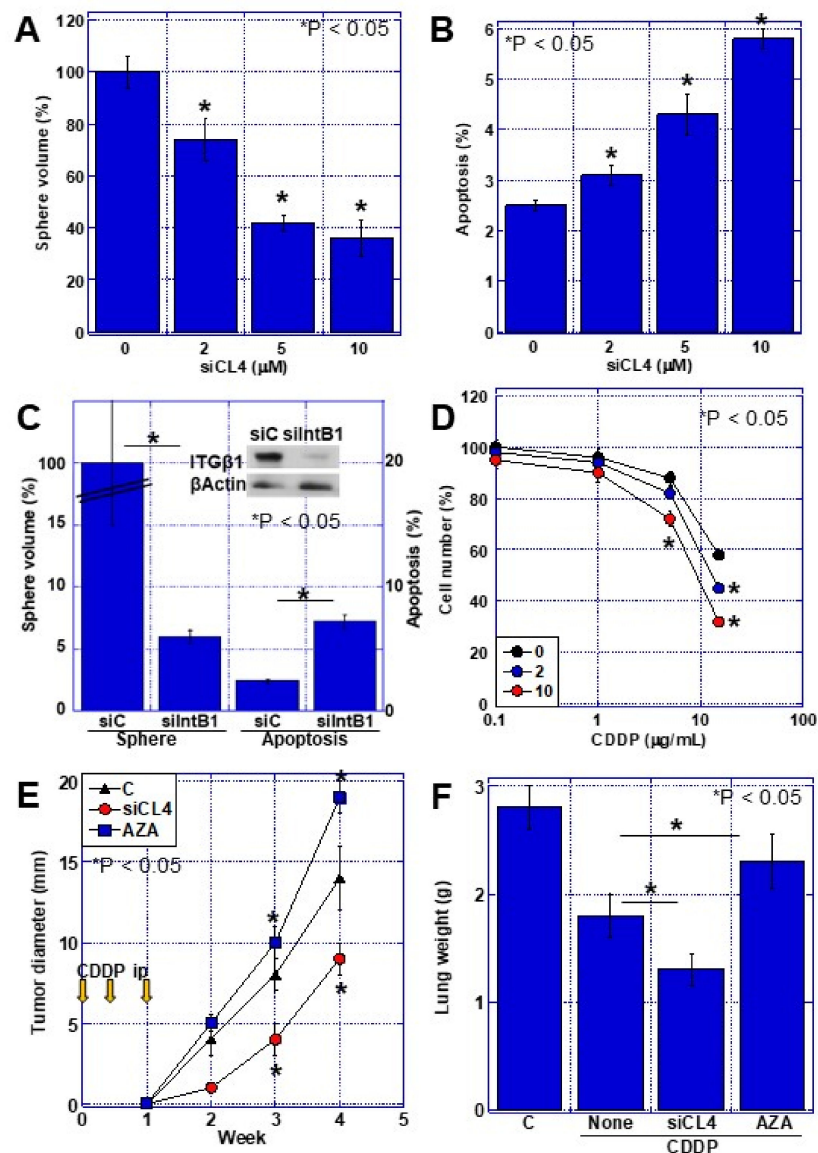


Figure 6. Effect of CLDN4-integrin $\beta 1$ interaction on malignant phenotypes in T24 BUC cells. (A) Effect of *CLDN4* knockdown on sphere formation. (B) Effect of *CLDN4* knockdown on apoptosis. (C) Effect of *ITGB1* knockdown on sphere formation and apoptosis. (D) Effect of *CLDN4* knockdown on chemosensitivity to CDDP. (E) Effect of CDDP on tumor growth of T24 cells pretreated with control vehicle (C), CLDN4 siRNA (siCL4), or 5-AZA (AZA). (F) Effect of CDDP on lung metastasis of T24 cells pretreated with control vehicle (C), CLDN4 siRNA (siCL4), or 5-AZA (AZA). Error bar indicates SD calculated by Student's *t*-test from three independent trials or 5 mice. CLDN, claudin; BUC, bladder urothelial carcinoma; si, short interference RNA; siC, control siRNA; siCL4, siRNA for CLDN4; siIntB1, siRNA for integrin $\beta 1$; ITGB1, integrin $\beta 1$; CDDP, cisplatin.

3. Discussion

Our analysis of human BUC cases revealed that *CLDN4* promoter DNA hypomethylation causes *CLDN4* overexpression in BUC. We also found that *CLDN4* overexpression increased non-tight junction *CLDN4* expression, resulting in increased stemness, likely via activation of integrin $\beta 1$, suppression of apoptosis, decrease in drug sensitivity, and promotion of tumor growth and metastasis.

The involvement of epigenetics in *CLDN* expression has been reported for *CLDN1* [16,20,21], *CLDN2* [22], *CLDN3* [23–25], *CLDN6* and *9* [26], *CLDN7* [27], and *CLDN11* [28]. Epigenetic involvement has also been reported for *CLDN4* [14,24], wherein,

similar to this study, *CLDN4* overexpression by promoter hypomethylation was reported in gastric cancer [14].

This study shows that decreased *CLDN4* promoter DNA methylation results in increased *CLDN4* expression. In our previous study, *CLDN4* overexpression correlated with cancer progression in BUC [3]. In this study, we also found a correlation between *CLDN4* promoter DNA hypomethylation and *CLDN4* overexpression and BUC grade or invasion. In cases with *CLDN4* promoter DNA hypomethylation, accelerated proliferation, increased stemness, and enhanced EMT phenotype were observed. Furthermore, *CLDN4* promoter DNA hypomethylation of BUC cell lines by 5-AZA treatment resulted in enhanced *CLDN4* expression, increased stemness, and a higher expression of anti-apoptotic factors. In contrast, knockdown of *CLDN4* showed the opposite results. In our previous report, *CLDN4* overexpression increased malignancy by promoting resistance to anticancer drugs [3]; however, our results show that *CLDN4* overexpression increases cancer malignant phenotypes in situations without usage of anticancer drugs.

Until now, *CLDN4* expression has been implicated as an epithelial marker, and its reduction suggests the EMT phenotype [29]. In this study, we examined the association between *CLDN4* overexpression and function of tight junctions. Interestingly, the excess expression of *CLDN4* above the expression level sufficient to retain tight junction function for TER generated a monomer of *CLDN4* that is not integrated into tight junctions. Furthermore, the non-tight junction *CLDN4* promoted stemness, EMT phenotype, proliferation, and anti-apoptotic survival. We have previously reported roles of non-tight junction *CLDN4*: FAK activation by *CLDN4* on the plasma membrane [5] and YAP activation by migration into the cytoplasm and nucleus [30,31]. The diversity of non-tight junction functions of *CLDN4* has attracted much attention [32], and our studies have shown that *CLDN4* overexpression is associated with malignant phenotypes in cancer cells through a variety of mechanisms.

Our results revealed that the increased BUC malignant phenotypes due to *CLDN4* overexpression is due to increased levels of non-tight junction *CLDN4*, which promotes stemness through the activation of integrin $\beta 1$. *CLDN7* has been previously reported to bind integrin $\beta 1$ and result in downstream FAK phosphorylation [19,33]. Moreover, we have previously shown that *CLDN4*, as well as *CLDN7*, binds to integrin $\beta 1$ and activates FAK in BUC in gastric cancer [5]. In this study, *CLDN4* showed approximately 40% of the affinity of *CLDN7* for integrin $\beta 1$. Integrin $\beta 1$ is known to promote stemness through downstream FAK activation [34,35]. Alterations in the association of cancer cells with the stroma [36] and Notch signaling have been reported as the underlying mechanisms [35]. In the present study, binding *CLDN4* to integrin $\beta 1$ resulted in FAK phosphorylation and increased sphere-forming capacity. As a result of this, we observed increased stemness, decreased apoptosis, increased drug resistance, and increased cancer metastatic potential.

In the present study, *CLDN4* promoter hypomethylation induced *CLDN4* overexpression in bladder cancer. However, the cause of the hypomethylation could not be clarified. BUC is associated with abnormal DNA methylation, and disruption of the methylation pattern establishment mechanism may result in deregulation of DNA methyltransferases and demethylases and altered metabolism of methyl groups [37]. In BUCs, several methyltransferases are upregulated [38–40]; their enhanced activity may result in depletion of methyl donors, thus potentially inducing an hypomethylation of gene promoters.

Thus, the results suggest that *CLDN4* promoter DNA hypomethylation is the cause of *CLDN4* overexpression in BUC, and that overexpression results in increased non-tight junction *CLDN4*, which promotes cancer stemness through integrin $\beta 1$ activation and consequent increased malignant potential. Furthermore, an increased *CLDN4* level correlates with tumor virulence through various mechanisms, including increased drug resistance by tight junction barrier function, increased EMT phenotype, and increased stemness. These findings suggest that *CLDN4* promoter DNA methylation may be a new marker of bladder cancer malignancy and may be applied to develop novel therapeutic targets.

4. Materials and Methods

4.1. Surgical Specimens

In total, 157 paired tissue samples of tumor and the corresponding normal-appearing tissue adjacent to the tumor were obtained from patients with BUC during the surgical procedure (transurethral resection or radical cystectomy). Corresponding normal-appearing tissues were judged macroscopically or endoscopically and dissected. Half of the tissues were used for pathological examination; if the tissue included cancer tissue, the section was excluded from the analyses. Control tissue samples of normal urothelia were obtained from patients without BUC. Tumors were staged according to the UICC TNM classification system [18]. All collected tissues were frozen and stored at $-80\text{ }^{\circ}\text{C}$ until use for DNA extraction.

As written informed consents were not obtained from the patients, any identifying information was removed from the samples prior to analysis in order to ensure strict privacy protection (unlinkable anonymization). All procedures were performed in accordance with the Ethical Guidelines for Human Genome/Gene Research issued by the Japanese Government and were approved by the Ethics Committee of Nara Medical University (approval number 937, 20 October 2010).

4.2. Cells and Reagents

T24, RT4, and UMUC3 human BUC cell lines were purchased from the American Type Culture Collection (ATCC; Manassas, VA, USA). Cells were cultured in Dulbecco's modified Eagle's medium supplemented with 10% fetal bovine serum at $37\text{ }^{\circ}\text{C}$ in 5% CO_2 . Cell growth was assessed using tetrazolium (MTT) dye assay as previously described [41]. CDDP was purchased from Novaplus (Bedford, OH, USA).

4.3. DNA Extraction

DNA was extracted using conventional extraction methods [42]. DNA ($2\text{ }\mu\text{g}$) was treated with sodium bisulfite using an Epitect Bisulfite Kit (Qiagen) according to the manufacturer's protocol and resuspended in $40\text{ }\mu\text{L}$ of distilled water for subsequent use.

4.4. The Primer Set for Pyrosequencing

The genomic sequences of *CLDN4* gene (NCBI Reference Sequence: NG_012868.1) obtained from the National Center for Biotechnology Information (NCBI). DataBase of CpG islands and Analytical Tool (DBCAT) was used to identify CpG sites. The primer set for pyrosequence was designed by PyroMark Assay Design Software 2.0 (Qiagen, Hilden, Germany). PCR primers were designed to include the -1457 CpG site, and their sequences are: forward: 5'-GAA TTG GAT ATA TAG TTA TTA GTG TTG-3' and reverse: 5'-CCA ACC ATA CTA AAA ACT CTA CA-3'. The sequencing primer was 5'-AGT TAT TAG TGT TGG ATA ATG-3' (synthesized by Sigma Genosys, Ishikari, Japan).

4.5. Bisulfite Pyrosequencing

DNA methylation status of *CLDN4* CpG sites was assessed by pyrosequencing using Pyrosequencing 96HS (Biotage, Uppsala, Sweden) and PyroMark Q24 (Qiagen) according to the manufacturer's protocol. Reaction volumes of $30\text{ }\mu\text{L}$ contained $5\times$ GoTaq buffer, 1.5 U GoTaq Hot Start Polymerase (Promega Biosciences, San Louis Obispo, CA, USA), $1\text{ }\mu\text{M}$ of primers, and 500 nM of dNTPs. PCR conditions were as follows: $95\text{ }^{\circ}\text{C}$ for 3 min; 35 cycles of $95\text{ }^{\circ}\text{C}$ for 30 s, $65\text{ }^{\circ}\text{C}$ for 30 s, and $72\text{ }^{\circ}\text{C}$ for 30 s, and a final extension step at $72\text{ }^{\circ}\text{C}$ for 4 min. The pyrosequenced product including the CpG region was assayed on the Illumina GoldenGate Panel.

4.6. Small Interfering RNA

Stealth Select RNAi (siRNA) targeting mouse *Hmgb1* and rat *Hmgb1* were purchased from Sigma (St. Louis, MO, USA). AllStars Negative Control siRNA was used as a control (Qiagen). The cells were transfected with 10 μ M of siRNA using Lipofectamine 3000 (Thermo Fisher, Tokyo, Japan) according to the manufacturer's recommendations.

4.7. Enzyme-Linked Immunosorbent Assay (ELISA)

ELISA kits were used for measuring protein concentrations of CLDN4, Ki-67, GNL3, CD44v9, SNAIL, and vimentin (Table 3), according to the manufacturer's instructions.

Table 3. Antibodies and ELISA kits used.

Antibody	Species	Provider	City and Country
CLDN4	human	clone 4D3	[3]
ZO-1	human	Abcam	Cambridge, MA, USA
ITG β 1	human	Santa-Cruz Biotechnology	Santa Cruz, CA, USA
pFAK (pTyr397)	human	Boster Immunoleader	Pleasanton, CA, USA
FAK	human	Santa-Cruz Biotechnology	Santa Cruz, CA, USA
Ki-67	human	DAKO-Agilent	Santa Clara, CA, USA
CD44v9	human	Cosmobio	Carlsbad, CA, USA
Nucleostemin	human	Santa-Cruz Biotechnology	Santa Cruz, CA, USA
E-cadherin	human	DAKO-Agilent	Santa Clara, CA, USA
β Actin	human	Zymed Laboratories Inc.	South San Francisco, CA, USA
ELISA	Species	Provider	City and country
CLDN4	human	MyBiosource, Inc.	San Diego, CA, USA
CLDN7	Human	Wuhan Huamei Biotech	Wuhan, China
Ki-67	human	Abcam	Cambridge, MA, USA
GNL3	human	antibodies-online GmbH	Aachen, Germany
CD44v9	human	Elabscience	Houston, TX, USA
CDH1	human	Abcam	Cambridge, MA, USA
SNAIL	human	Biocompare	South San Francisco, CA, USA
Vimentin	human	Abcam	Cambridge, MA, USA

4.8. Immunohistochemistry

Consecutive sections of 4 μ m of BUC tissues were immunohistochemically stained using 0.2 μ g/mL of primary antibodies using a previously described immunoperoxidase technique [39]. Secondary antibodies (peroxidase-conjugated antibodies, MBL, Nagoya, Japan) were used at a concentration of 0.2 μ g/mL. Tissue sections were color-developed with diamine benzidine hydrochloride (DAKO, Glostrup, Denmark) and counterstained with Meyer's hematoxylin (Sigma). The primary antibodies used are listed in Table 3.

4.9. Protein Extraction

For preparing whole cell lysate, BUC cells were washed twice with cold phosphate-buffered saline, harvested, and lysed with 0.1% sodium dodecyl sulfate (SDS), 0.5% Tween 20-, or 0.5% perfluoro-octanoic acid (PFO)-added RIPA-buffer (Thermo Fisher Scientific, Tokyo, Japan) supplemented with protease inhibitor cocktail (Promega) [43]. SDS solubilizes whole CLDN4 protein, Tween-20 solubilizes the CLDN4 monomer, i.e., non-tight junction CLDN4, and PFO solubilizes CLDN4 polymer, i.e., tight junction CLDN4 [44]. Protein assay was performed using a Protein Assay Rapid Kit (Wako Pure Chemical, Osaka, Japan).

4.10. Immunoblot Analysis

Whole-cell lysates of BUC cells were prepared as previously described [43]. Lysates (20 µg) were subjected to immunoblot analysis using SDS polyacrylamide gel electrophoresis (12.5%), followed by electrotransfer onto nitrocellulose filters. The filters were incubated with primary antibodies (diluted to 1/500 by 1x tris buffered saline with Tween 20 [TBS-T20, Thermo Fisher Pierce, Tokyo, Japan]) for 120 min at room temperature, and then washed with TBS-T20 3 times at room temperature. The filters were incubated with primary antibodies (diluted to 1/500 by 1x tris buffered saline with tween 20 [TBS-T20, Thermo Fisher Pierce, Tokyo, Japan]) for 120 min at room temperature, and then washed with TBS-T20 3 times at room temperature. Filtered were incubated with peroxidase-conjugated IgG antibodies (MBL, diluted to 1/200 by TBS-T20) for 120 min at room temperature, and then washed with TBS-T20 3 times at room temperature. Anti-tubulin antibody was used to assess the levels of protein loaded per lane (Oncogene Research, Cambridge, MA, USA). The immune complex was visualized using an Enhanced Chemiluminescence Western-blot detection system (Amersham, Aylesbury, UK). The primary antibodies used are listed in Table 3. Images were captured on a computer and the signal strength was measured using NIH ImageJ software (version 1.52, Bethesda, MD, USA).

4.11. Immunoprecipitation

Immunoprecipitation was performed according to a method described previously [45]. Lysates were pre-cleaned in lysis buffer with protein A/G agarose (Santa Cruz) for 1 h at 4 °C and subsequently centrifuged. The supernatants were incubated with a precipitation antibody [either against ZO-1 or CLDN4 (4D3)] and protein A/G agarose for 3 h at 4 °C. Precipitates were collected via centrifugation, washed five times with lysis buffer, solubilized with sample buffer (Sigma, 40 µg), and subjected to an immunoblot analysis with antibodies against CLDN4 (4D3), integrin β1, and/or ZO-1. The antibodies used are listed in Table 3.

4.12. Affinity Assay

Recombinant human integrin β1 (Abcam, Cambridge, UK, the used amount is shown in Figure 5D) was mixed with recombinant human CLDN4 (Abcam) or recombinant human CLDN7 (Cloud Cone, Tokyo, Japan) in equal amounts in a binding buffer containing 20 mM of Tris-HCl, 150 mM of NaCl, 1 mM of CaCl₂, and 35 mg/mL of bovine serum albumin and incubated for 2 h at 30 °C. The reaction solution was subjected to immunoprecipitation with anti-integrin β1 antibody. CLDN4 or CLDN7 in the immunoprecipitant was measured by ELISA kit. The antibodies and ELISA kits used are listed in Table 3.

4.13. Reverse Transcription-Polymerase Chain Reaction (RT-PCR)

To assess human *CLDN4* mRNA expression, RT-PCR was performed with 0.5 µg of total RNA extracted from BUC cells using an RNeasy kit (Qiagen). The primer sets used are shown in Table 4. Primers were synthesized by Sigma Genosys. The *GAPDH* mRNA was also amplified for use as an internal control.

Table 4. Primer sets used.

Gene Symbol	Species	Accession No.	Site	Sequence
<i>CLDN4</i>	human	NM_001305.4	Upper	CTC CAT GGG GCT ACA GGT AA
			Lower	AGC AGC GAG TCG TAC ACC TT
<i>GNL3</i>	human	BC001024.2	Upper	ATT GCC AAC AGT GGT GTT CA
			Lower	AAT GGC TTT GCT GCA AGT TT
<i>BCL2</i>	human	M13994.1	Upper	ACG ACA ACC GGG AGA TAG TG
			Lower	CAT CCC AGC CTC CGT TAT CC

Table 4. *Cont.*

Gene Symbol	Species	Accession No.	Site	Sequence
BAX	human	L22473.1	Upper Lower	CAT GAA GAC AGG GGC CCT TT CTT CCA GAT GGT GAG CGA GG
GAPDH	human	BC025925.1	Upper Lower	GAG TCA ACG GAT TTG GTC GT TTG ATT TTG GAG GGA TCT CG

4.14. Sphere Assay

Cells (1000 cells per well) were seeded onto uncoated bacteriological 35-mm dish (Corning, Corning, NY, USA) with 3D Tumorsphere Medium XF (Sigma). After 7 days, sphere images were captured on a computer, and the sphere volume was measured using NIH ImageJ software (version 1.52, Bethesda, MD, USA).

4.15. Apoptosis Assay

Apoptosis was assessed via the examination of 1000 cells, which were stained with Hoechst 33342 dye (Life Technologies, Carlsbad, CA, USA), and viewed using a fluorescent microscope.

4.16. Transepithelial Electroresistance (TER) Assay

The cellZscope tight junction monitoring system (Fujifilm, Tokyo, Japan) was used to measure the TER of the cells. Briefly, 1×10^5 cells were seeded onto the provided insert and allowed to form multiple cell layers. Thereafter, the TER was measured using the system as per the manufacturer's instructions. A negative control was generated, in which tight junction formation was impaired via treatment with cytochalasin B (CB; 10 μ M, Wako).

4.17. Animals

Four-week-old male BALB/c Slc-nu/nu mice were procured from SLC Japan (Shizuoka, Japan). The mice were maintained according to the institutional guidelines approved by the Committee for Animal Experimentation of Nara Medical University, in accordance with the current regulations and standards of the Ministry of Health, Labor, and Welfare (Approval no. 11356, 1 February 2016).

4.18. Animal Tumor Models

To establish a subcutaneous tumor model, T24 cancer cells (1×10^7) were inoculated into the scapular subcutaneous tissues of nude mice (5 mice in each group). For the lung metastasis model, T24 cancer cells (1×10^6) were inoculated into the caudal vein (5 mice in each group). The lungs of the mice were observed for 4 weeks following inoculation. The lungs were sliced into 2 mm thick sections and the metastatic foci were counted under a stereomicroscope (Nikon, Tokyo, Japan). CDDP (3 mg/kg) was administered into the peritoneal cavity on days 1, 3, and 7.

4.19. Statistical Analysis

Statistical significance was calculated using the chi-squared test, Fisher's square test, and Kruskal–Wallis test with InStat software (GraphPad, Los Angeles, CA, USA). Statistical significance was defined as a two-sided *p*-value of <0.05.

Author Contributions: Conceptualization, H.K.; investigation, F.M., M.K. (Masaomi Kuwada), S.H., S.M. and T.M.; resources, M.M., Y.N., U.K.B., Y.L. and M.K. (Masuo Kondoh); data curation, F.M., M.K. (Masaomi Kuwada), S.K., R.F.-T., K.F. (Kiyomu Fujii), H.O. and T.O.; writing—original draft preparation, F.M. and M.K. (Masaomi Kuwada); writing—review and editing, H.K.; supervision, N.T., M.K. (Masuo Kondoh) and K.F. (Kiyohide Fujimoto); funding acquisition, R.F.-T., H.K., S.K. and S.M. All authors have read and agreed to the published version of the manuscript.

Funding: This work was supported by MEXT KAKENHI Grant Numbers 19K16564 (R.F.-T.), 20K21659 (H.K.), 20K18007 (S.K.), and 21K10143 (S.M.).

Institutional Review Board Statement: As written informed consents were not obtained from the patients, any identifying information was removed from the samples prior to analysis in order to ensure strict privacy protection (unlinkable anonymization). All procedures were performed in accordance with the Ethical Guidelines for Human Genome/Gene Research issued by the Japanese Government and were approved by the Ethics Committee of Nara Medical University (approval number 937, 20 October 2010). The mice were maintained according to the institutional guidelines approved by the Committee for Animal Experimentation of Nara Medical University, in accordance with the current regulations and standards of the Ministry of Health, Labor, and Welfare (Approval no. 11356, 1 February 2016).

Informed Consent Statement: Not applicable.

Data Availability Statement: Not applicable.

Acknowledgments: The authors thank Tomomi Masutani for expert assistance with the preparation of this manuscript.

Conflicts of Interest: The authors declare no conflict of interest.

Abbreviations

TJ	tight junction
CLDN4	claudin-4
BUC	bladder urothelial carcinoma
EMT	epithelial-mesenchymal transition
AZA	aza-2'-deoxycytidine
SDS	sodium dodecyl sulfate
T20	tween 20
TER	transepithelial electric resistance
PFO	perfluoro-octanoic acid
CDDP	cisplatin

References

- Turksen, K.; Troy, T.C. Junctions gone bad: Claudins and loss of the barrier in cancer. *Biochim. Biophys. Acta* **2011**, *1816*, 73–79. [[CrossRef](#)] [[PubMed](#)]
- Escudero-Esparza, A.; Jiang, W.G.; Martin, T.A. The Claudin family and its role in cancer and metastasis. *Front. Biosci.* **2011**, *16*, 1069–1083. [[CrossRef](#)] [[PubMed](#)]
- Kuwada, M.; Chihara, Y.; Luo, Y.; Li, X.; Nishiguchi, Y.; Fujiwara, R.; Sasaki, T.; Fujii, K.; Ohmori, H.; Fujimoto, K.; et al. Pro-chemotherapeutic effects of antibody against extracellular domain of claudin-4 in bladder cancer. *Cancer Lett.* **2015**, *369*, 212–221. [[CrossRef](#)] [[PubMed](#)]
- Fujiwara-Tani, R.; Sasaki, T.; Luo, Y.; Goto, K.; Kawahara, I.; Nishiguchi, Y.; Kishi, S.; Mori, S.; Ohmori, H.; Kondoh, M.; et al. Anti-claudin-4 extracellular domain antibody enhances the antitumoral effects of chemotherapeutic and antibody drugs in colorectal cancer. *Oncotarget* **2018**, *9*, 37367–37378. [[CrossRef](#)]
- Nishiguchi, Y.; Fujiwara-Tani, R.; Sasaki, T.; Luo, Y.; Ohmori, H.; Kishi, S.; Mori, S.; Goto, K.; Yasui, W.; Sho, M.; et al. Targeting claudin-4 enhances CDDP-chemosensitivity in gastric cancer. *Oncotarget* **2019**, *10*, 2189–2202. [[CrossRef](#)]
- Sasaki, T.; Fujiwara-Tani, R.; Kishi, S.; Mori, S.; Luo, Y.; Ohmori, H.; Kawahara, I.; Goto, K.; Nishiguchi, Y.; Mori, T.; et al. Targeting claudin-4 enhances chemosensitivity of pancreatic ductal carcinomas. *Cancer Med.* **2019**, *8*, 6700–6708. [[CrossRef](#)]
- Swishhelm, K.; Macek, R.; Kubbies, M. Role of claudins in tumorigenesis. *Adv. Drug Deliv. Rev.* **2005**, *57*, 919–928. [[CrossRef](#)]
- Kwon, M.J. Emerging roles of claudins in human cancer. *Int. J. Mol. Sci.* **2013**, *14*, 18148–18180. [[CrossRef](#)]
- Fumarola, S.; Cecati, M.; Sartini, D.; Ferretti, G.; Milanese, G.; Galosi, A.B.; Pozzi, V.; Campagna, R.; Morresi, C.; Emanuelli, M.; et al. Bladder Cancer Chemosensitivity is Affected by Paraoxonase-2 Expression. *Antioxidants* **2020**, *9*, 175. [[CrossRef](#)]
- Cavalli, G.; Heard, E. Advances in epigenetics link genetics to the environment and disease. *Nature* **2019**, *571*, 489–499. [[CrossRef](#)]
- Feinberg, A.P. The Key Role of Epigenetics in Human Disease Prevention and Mitigation. *N. Eng. J. Med.* **2018**, *378*, 1323–1334. [[CrossRef](#)] [[PubMed](#)]
- Kanwal, R.; Gupta, K.; Gupta, S. Cancer epigenetics: An introduction. *Methods Mol. Biol.* **2015**, *1238*, 3–25. [[PubMed](#)]
- Nebbioso, A.; Tambaro, F.P.; Dell'Aversana, C.; Altucci, L. Cancer epigenetics: Moving forward. *PLoS Genet.* **2018**, *14*, e1007362. [[CrossRef](#)] [[PubMed](#)]
- Kwon, M.J.; Kim, S.H.; Jeong, H.M.; Jung, H.S.; Kim, S.S.; Lee, J.E.; Gye, M.C.; Erkin, O.C.; Koh, S.S.; Choi, Y.L.; et al. Claudin-4 overexpression is associated with epigenetic derepression in gastric carcinoma. *Lab. Invest.* **2011**, *91*, 1652–1667. [[CrossRef](#)]

15. Boireau, S.; Buchert, M.; Samuel, M.S.; Pannequin, J.; Ryan, J.L.; Choquet, A.; Chapuis, H.; Rebillard, X.; Avances, C.; Ernst, M.; et al. DNA-methylation-dependent alterations of claudin-4 expression in human bladder carcinoma. *Carcinogenesis* **2007**, *28*, 246–258. [[CrossRef](#)]
16. Hahn-Stromberg, V.; Askari, S.; Ahmad, A.; Befekadu, R.; Nilsson, T.K. Expression of claudin 1, claudin 4, and claudin 7 in colorectal cancer and its relation with CLDN DNA methylation patterns. *Tumour Biol.* **2017**, *39*, 1010428317697569. [[CrossRef](#)]
17. Litkouhi, B.; Kwong, J.; Lo, C.M.; Smedley, J.G., 3rd; McClane, B.A.; Aponte, M.; Gao, Z.; Sarno, J.L.; Hinnners, J.; Welch, W.R.; et al. Claudin-4 overexpression in epithelial ovarian cancer is associated with hypomethylation and is a potential target for modulation of tight junction barrier function using a C-terminal fragment of Clostridium perfringens enterotoxin. *Neoplasia* **2007**, *9*, 304–314. [[CrossRef](#)]
18. Edge, S.; Byrd, D.R.; Compton, C.C.; Fritz, A.G.; Greene, F.L.; Trotti, A. *AJCC Cancer Staging Manual*, 7th ed.; Springer: New York, NY, USA, 2010.
19. Lu, Z.; Kim, D.H.; Fan, J.; Lu, Q.; Verbanac, K.; Ding, L.; Renegar, R.; Chen, Y.H. A non-tight junction function of claudin-7-Interaction with integrin signaling in suppressing lung cancer cell proliferation and detachment. *Mol. Cancer* **2015**, *14*, 120. [[CrossRef](#)]
20. Hasegawa, K.; Wakino, S.; Simic, P.; Sakamaki, Y.; Minakuchi, H.; Fujimura, K.; Hosoya, K.; Komatsu, M.; Kaneko, Y.; Kanda, T.; et al. Renal tubular Sirt1 attenuates diabetic albuminuria by epigenetically suppressing Claudin-1 overexpression in podocytes. *Nat. Med.* **2013**, *19*, 1496–1504. [[CrossRef](#)]
21. Di Cello, F.; Cope, L.; Li, H.; Jeschke, J.; Wang, W.; Baylin, S.B.; Zahnow, C.A. Methylation of the claudin 1 promoter is associated with loss of expression in estrogen receptor positive breast cancer. *PLoS ONE* **2013**, *8*, e68630.
22. Hichino, A.; Okamoto, M.; Taga, S.; Akizuki, R.; Endo, S.; Matsunaga, T.; Ikari, A. Down-regulation of Claudin-2 Expression and Proliferation by Epigenetic Inhibitors in Human Lung Adenocarcinoma A549 Cells. *J. Biol. Chem.* **2017**, *292*, 2411–2421. [[CrossRef](#)] [[PubMed](#)]
23. Zhang, Z.; Yu, W.; Chen, S.; Chen, Y.; Chen, L.; Zhang, S. Methylation of the claudin3 promoter predicts the prognosis of advanced gastric adenocarcinoma. *Oncol. Rep.* **2018**, *40*, 49–60. [[PubMed](#)]
24. Kwon, M.J.; Kim, S.S.; Choi, Y.L.; Jung, H.S.; Balch, C.; Kim, S.H.; Song, Y.S.; Marquez, V.E.; Nephew, K.P.; Shin, Y.K. Derepression of CLDN3 and CLDN4 during ovarian tumorigenesis is associated with loss of repressive histone modifications. *Carcinogenesis* **2010**, *31*, 974–983. [[CrossRef](#)] [[PubMed](#)]
25. Honda, H.; Pazin, M.J.; D'Souza, T.; Ji, H.; Morin, P.J. Regulation of the CLDN3 gene in ovarian cancer cells. *Cancer Biol. Ther.* **2007**, *6*, 1733–1742. [[CrossRef](#)]
26. Nishikiori, N.; Sawada, N.; Ohguro, H. Prevention of murine experimental corneal trauma by epigenetic events regulating claudin 6 and claudin 9. *JPN J. Ophthalmol.* **2008**, *52*, 195–203. [[CrossRef](#)]
27. Kudinov, A.E.; Deneka, A.; Nikonova, A.S.; Beck, T.N.; Ahn, Y.H.; Liu, X.; Martinez, C.F.; Schultz, F.A.; Reynolds, S.; Yang, D.H.; et al. Musashi-2 (MSI2) supports TGF- β signaling and inhibits claudins to promote non-small cell lung cancer (NSCLC) metastasis. *Proc. Natl. Acad. Sci. USA* **2016**, *113*, 6955–6960. [[CrossRef](#)]
28. Li, J.; Zhou, C.; Ni, S.; Wang, S.; Ni, C.; Yang, P.; Ye, M. Methylated claudin-11 associated with metastasis and poor survival of colorectal cancer. *Oncotarget* **2017**, *8*, 96249–96262. [[CrossRef](#)]
29. Kyuno, D.; Yamaguchi, H.; Ito, T.; Kono, T.; Kimura, Y.; Imamura, M.; Konno, T.; Hirata, K.; Sawada, N.; Kojima, T. Targeting tight junctions during epithelial to mesenchymal transition in human pancreatic cancer. *World J. Gastroenterol.* **2014**, *20*, 10813–10824. [[CrossRef](#)]
30. Nakashima, C.; Yamamoto, K.; Kishi, S.; Sasaki, T.; Ohmori, H.; Fujiwara-Tani, R.; Mori, S.; Kawahara, I.; Nishiguchi, Y.; Mori, T.; et al. Clostridium perfringens enterotoxin induces claudin-4 to activate YAP in oral squamous cell carcinomas. *Oncotarget* **2020**, *11*, 309–321. [[CrossRef](#)]
31. Fujiwara-Tani, R.; Fujii, K.; Mori, S.; Kishi, S.; Sasaki, T.; Ohmori, H.; Nakashima, C.; Kawahara, I.; Nishiguchi, Y.; Mori, T.; et al. Role of Clostridium perfringens Enterotoxin on YAP Activation in Colonic Sessile Serrated Adenoma/Polyps with Dysplasia. *Int. J. Mol. Sci.* **2020**, *21*, 3840. [[CrossRef](#)]
32. Fredriksson, K.; Van Itallie, C.M.; Aponte, A.; Gucek, M.; Tietgens, A.J.; Anderson, J.M. Proteomic analysis of proteins surrounding occludin and claudin-4 reveals their proximity to signaling and trafficking networks. *PLoS ONE* **2015**, *10*, e0117074. [[CrossRef](#)] [[PubMed](#)]
33. Kim, D.H.; Lu, Q.; Chen, Y.H. Claudin-7 modulates cell-matrix adhesion that controls cell migration, invasion and attachment of human HCC827 lung cancer cells. *Oncol. Lett.* **2019**, *17*, 2890–2896. [[CrossRef](#)] [[PubMed](#)]
34. Gardelli, C.; Russo, L.; Cipolla, L.; Moro, M.; Andriani, F.; Rondinone, O.; Nicotra, F.; Sozzi, G.; Bertolini, G.; Roz, L. Differential glycosylation of collagen modulates lung cancer stem cell subsets through β 1 integrin-mediated interactions. *Cancer Sci.* **2021**, *112*, 217–230. [[CrossRef](#)]
35. Moon, J.H.; Rho, Y.S.; Lee, S.H.; Koo, B.S.; Lee, H.J.; Do, S.I.; Cho, J.H.; Eun, Y.G.; Park, M.W.; Shin, H.A.; et al. Role of integrin β 1 as a biomarker of stemness in head and neck squamous cell carcinoma. *Oral. Oncol.* **2019**, *96*, 34–41. [[CrossRef](#)] [[PubMed](#)]
36. Schulz, W.A. DNA methylation in urological malignancies. *Int. J. Oncol.* **1998**, *13*, 151–167.
37. Wang, C.; Jiang, X.; Huang, B.; Zhou, W.; Cui, X.; Zheng, C.; Liu, F.; Bi, J.; Zhang, Y.; Luo, H.; et al. Inhibition of matrix stiffness relating integrin β 1 signaling pathway inhibits tumor growth in vitro and in hepatocellular cancer xenografts. *BMC Cancer* **2021**, *21*, 1276. [[CrossRef](#)]

38. Campagna, R.; Pozzi, V.; Spinelli, G.; Sartini, D.; Milanese, G.; Galosi, A.B.; Emanuelli, M. The Utility of Nicotinamide N-Methyltransferase as a Potential Biomarker to Predict the Oncological Outcomes for Urological Cancers: An Update. *Biomolecules* **2021**, *11*, 1214. [[CrossRef](#)]
39. Zhang, J.; Zhu, Y.; Wang, Y.; Fu, Q.; Xie, H.; Liu, Z.; Fu, H.; Cao, Y.; Xu, J.; Dai, B. Prognostic and Predictive Value of O(6)-methylguanine Methyltransferase for Chemotherapy in Patients with Muscle-Invasive Bladder Cancer. *Ann. Surg. Oncol.* **2018**, *25*, 342–348. [[CrossRef](#)]
40. Pozzi, V.; Di Ruscio, G.; Sartini, D.; Campagna, R.; Seta, R.; Fulvi, P.; Vici, A.; Milanese, G.; Brandoni, G.; Galosi, A.B.; et al. Clinical performance and utility of a NNMT-based urine test for bladder cancer. *Int. J. Biol. Markers* **2018**, *33*, 94–101. [[CrossRef](#)]
41. Kuniyasu, H.; Yano, S.; Sasaki, T.; Sasahira, T.; Sone, S.; Ohmori, H. Colon cancer cell-derived high mobility group 1/amphoterin induces growth inhibition and apoptosis in macrophages. *Am. J. Pathol.* **2005**, *166*, 751–760. [[CrossRef](#)]
42. Kuniyasu, H.; Luo, Y.; Fujii, K.; Sasahira, T.; Moriwaka, Y.; Tatsumoto, N.; Sasaki, T.; Yamashita, Y.; Ohmori, H. CD10 enhances metastasis of colorectal cancer by abrogating the anti-tumoural effect of methionine-enkephalin in the liver. *Gut* **2010**, *59*, 348–356. [[CrossRef](#)] [[PubMed](#)]
43. Kuniyasu, H.; Oue, N.; Wakikawa, A.; Shigeishi, H.; Matsutani, N.; Kuraoka, K.; Ito, R.; Yokozaki, H.; Yasui, W. Expression of receptors for advanced glycation end-products (RAGE) is closely associated with the invasive and metastatic activity of gastric cancer. *J. Pathol.* **2002**, *196*, 163–170. [[CrossRef](#)] [[PubMed](#)]
44. Mitic, L.L.; Unger, V.M.; Anderson, J.M. Expression, solubilization, and biochemical characterization of the tight junction transmembrane protein claudin-4. *Protein Sci.* **2003**, *12*, 218–227. [[CrossRef](#)] [[PubMed](#)]
45. Kuniyasu, H.; Oue, N.; Tsutsumi, M.; Tahara, E.; Yasui, W. Heparan Sulfate Enhances Invasion by Human Colon Carcinoma Cell Lines through Expression of CD44 Variant Exon 3. *Clin. Cancer Res.* **2001**, *7*, 4067–4072.